ISSN: 0067-2904

Synthesizing, Characterization, Studying Antioxidant and Anticancer of Some Metal Complexes with New 7-(3-Hydroxy-phenylazo)-quinoline-8-ol Ligand

Noor T.A. Al-rubaye*, Abbas Ali Salih Al –Hamdani
Department of Chemistry, College of Science for Women, University of Baghdad, Iraq

Received: 26/11/2024 Accepted: 29/ 4/2025 Published: 30/3/2026

Abstract

A new azo dye was synthesized by coupling the diazonium salt derived from 3-aminophenol with 8-hydroxyquinoline.This dye served as a precursor for synthesizing coordination complexes with manganese, chromium, molybdenum and vanadium. The ligand was characterized using ^{1}H and ^{13}C NMRspectroscopy, whilethe synthesized materials were characterized by MS, IR and UV-Vis spectrometry, thermogravimetric analysis,and elemental analysis. For the metal complexes, additional measurements such asconductivity, magnetic susceptibility, metal content and chlorine of the complexes were also measured. The results showed that the ligand behaves as trigonal behavior, and that the complexes adopt an octahedral geometry, except for thevanadium square pyramid thatwas given, whichalso showed that the complexes non-electrolytes. The effectiveness of the compounds in inhibiting free radicals was evaluated by the ability to act as an antioxidant which was measured using DPPH as a free radical and Gallic acid as a standard, and the IC_{50} value was determined. Vanadium and molybdenum complexes were evaluated as anticancer agents for the MCF-7 breast cancer cell line. The vanadium complex gave 97.62 µg/ml, the molybdenum complex gave a higher inhibition value than vanadium.

Keywords: Azo dyecomplexes,Antioxidant, Anticancer,8-Hydroxyquinoline,Thermal analysis.

تحضير، تشخيص، دراسة مضادات الاكسدة ومضادات السرطان لمعقدات بعض ايونات الفلزات مع اليكاند الجديد7-(3- هيدروكسي-فنيل ازو)-كوينولين-8-اول

نور طلال علي الربيعي*,عباس علي صالح الحمداني
قسم الكيمياء, كلية العلوم للبنات, جامعة بغداد, بغداد,العراق

الخلاصة

تم تحضير صبغة آزو جديدة عن طريق اقتران ملح الديازونيوم المشتق من 3- امينو فينول مع 8- هيدروكسي كوينولين. أستخدمت هذه الصبغة كمواد اولية لتحضير معقدات تناسقية مع المنغنيز والكروم والموليبدينوم والفناديوم. شخص الليكاند باستخدام مطيافية الرنين النووي المغناطيسي بينما شخصت المركبات المحضرة باستخدام مطيافية الكتلة والاشعة تحت الحمراء وفوق البنفسجية –المرئية والتحليل الحراري الوزني والتحليل الدقيق للعناصر اما بالنسبة للمعقدات المعدنية ، فقد تم قياس التوصيلة والحساسية المغناطيسية

*Email: noor.ali2305m@csw.uobaghdad.edu.iq

ومحتوى الفلز ومحتوى الكلور اضافة الى القياسات الاخرى. أظهرت النتائج أن الليكاند يسلك سلوك، وأن المعقدات تتخذ شكلًا هندسيًا ثماني السطوح، باستثناء الفناديوم هرم المربع القاعد، والذي أظهر أيضًا أن المعقدات غير إلكتروليتية. قُيِّمت فعالية المركبات في تثبيط الجذور الحرة من خلال قدرتها كمضاد للأكسدة، والتي قيست باستخدام DPPH كجذر حر وحمض الغاليك للمعايرة، وحُدِّدت قيمة IC_{50}. قُيِّمت معقدات الفاناديوم والموليبدينوم كعوامل مضادة للسرطان لسلالة خلايا سرطان الثدي MCF−7. أعطى معقد الفاناديوم 97.62 ميكروغرام/مل، بينما أعطى معقد الموليبدينوم قيمة تثبيط أعلى من الفاناديوم.

Introduction

Azo dyes represent a significant class of coordination compounds characterized by the presence of an azo group (-N=N-), which enables the formation of stable complexes with various metal ions. The unique properties of these ligands, combined with their ability to form multi-dentate structures, enhance their coordination chemistry and expand their applications across different fields, including pharmaceuticals, materials science, and environmental chemistry[1-2]. The versatility of azo ligands arises from their capacity to bind with transition metals such as Mn(II),Cr(III), Mo(VI) and V(IV),resulting in complexes that exhibit remarkable biological activities[3].Recent advances in research have underscored the biological significance of metal complexes formed with azo ligands, particularly in exploring their therapeutic potential for anticancer, antimicrobial, and anti-inflammatory properties, making them promising candidates for drug development [4-5]. Furthermore, the interaction between azo metal complexes and biological macromolecules, such as DNA and proteins, has been extensively investigated, providing insights into their mechanisms of action and therapeutic potentials[6]. The present study aims to address this gap by synthesizing novel metal ion complexes with newly developed azo ligands. By employing various characterization techniques, including UV-Vis spectroscopy, Fourier-transform infrared spectroscopy (FTIR), and thermogravimetric analysis (TGA), this research will elucidate the structural and thermal properties of the synthesized complexes[7]. Additionally, their antioxidant activities and interactions with biological targets will be evaluated[8-10].The primary objective of this study is to advance coordination chemistry by investigating new azo ligand and their metal complexes. The findings are expected to pave the way for the development of innovative therapeutic agents and functional materials that leverage the unique properties of azo compounds. This research includes preparing the azo dye ligand and using it to prepare metal ionic complexes for (V(IV), Cr(III), Mn(II), Mo(VI)), analyzing and diagnosing them using available methods, and evaluating their effectiveness as antioxidants and anti-cancers, in addition to studying them thermally and determining their thermal constants.

Material and Methods:

All components, chemicals and reagents, were sourced from commercial suppliers Sigma and Merck, withmetal ions identified as M-O through gravimetric methods. Molar conductivity was determined using aconductivity meter W-T-W, 25 °C. 1×10^{-3} M. Solvents such as DMSO-d_6 were used. Mass Spectrometry (MS) Q-P-50-A-D-I Analysis Mass spectra of various compounds were collected using a Shimadzu QP(E170Ev)-2010 Plus mass spectrometer. UV-Vis absorption spectra were obtained using a Shimadzu UV-1800 spectrophotometer. ^{1}H and ^{13}C NMR spectra were obtained using a Brucker (400MHz) spectrometer. Fourier transform infrared (FTIR) spectra were examined using IR Prestige-21. The instruments used were Bruker 4000-500 cm^{-1} and Shimadzu 4000-200 cm^{-1}. Metals were identified using theShimadzu (F.A.A) 680 G atomic clock. Magnetic properties were used with theequilibrium magnetic susceptibility model MSR-MKI. All previous types of thermal analysis were performed using Perkin-Elmer Pyris Diamond DSC/TGA.

Synthesis of azo dye ligand: [7-(3-Hydroxy-phenylazo)-quinoline-8-ol]

3-Aminophenol(1g,9.160mmol) was dissolved in a chilled mixture of 15 mL ethanol and 10 mL distilled water at 0–5°C. The temperature was maintained at 5°C.Then3ml of concentrated HClandNaNO$_2$(0.63200g, 9.160 mmoldissolved in cold distilled water) were added gradually. After 45 minutes of stirring, (8-hydroxyquinoline (1.32800 g, 9.160mmoldissolved in 20 mL of ethanol) was introduced to the diazonium. After stirring for 30 minutes for the reaction, the solution was observed to turn reddish brown. The product was collected after filtration and drying. The melting point was (162-165) °C, there was a brown precipitate, and the yield was 88%. Scheme 1 shows the formation of the ligand azo dye.

Synthesis of Metal Complexes:

15ml of the Azo ligand H_2L (1g, 0.00376mmol), was mixed with (0.00752g) of NaOH dissolved in water.After 10 minutes of continuous stirring,0.00376 mmol of the metal salt is added after dissolved in 15ml of water (0.00376mmol)[$VOSO_4.5H_2O$, 0.1g,$(NH_4)_2MoO_4$ 0.7g, $MnCl_2.4H_2O$0.7g, and$CrCl_3.6H_2O$1g].The solid complex was refluxed at 40°C for 4 hours under continuous heating. All unreacted components were separated and eliminated by briefly immersing the solid complex in hot ethanol. The complexes were collected, dried and weighed. The formation of the metal ion complexes is shown in Scheme1.

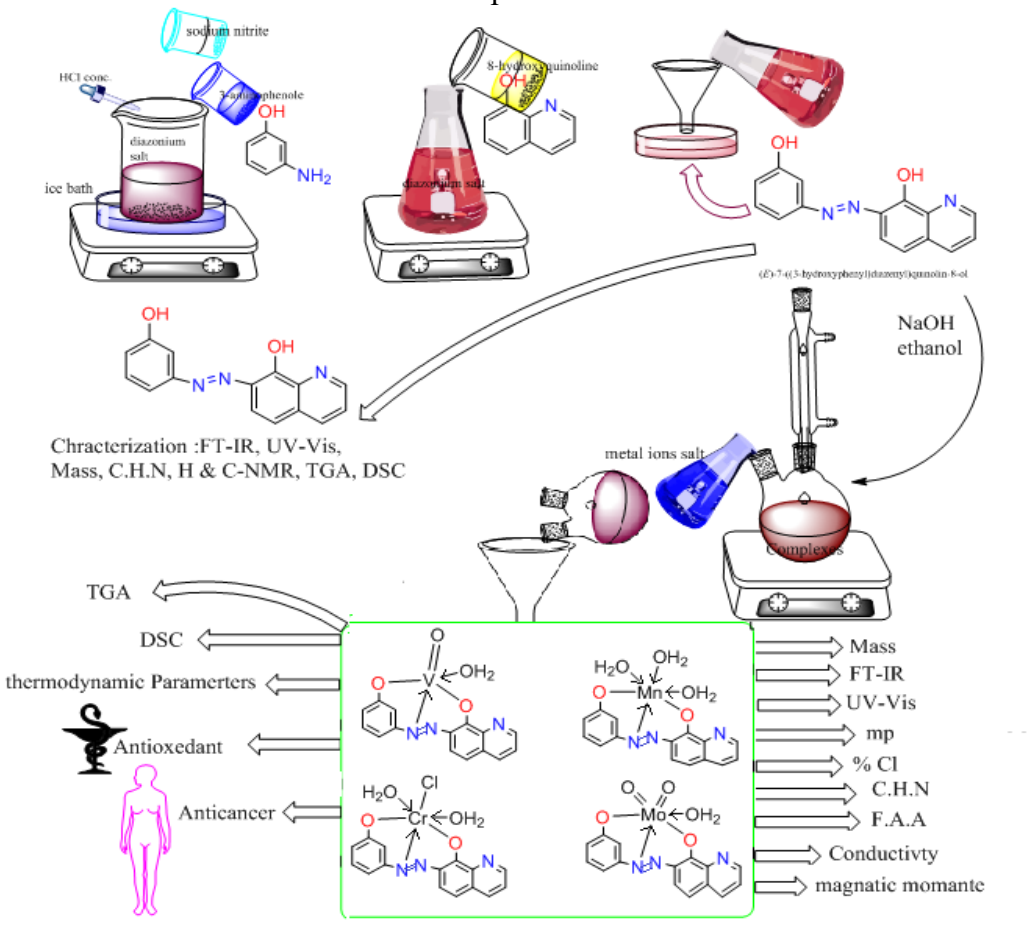

Scheme1: Formation for the ligand (H_2L) along with its metal complexes

Result and Discussion

Elementalanalysisof the ligand (H_2L) and the synthesized complexes

The synthetic compounds depicted in Scheme 1 were produced by reacting metal salts with the ligand. Elemental analysis results indicate that all compounds exhibit a 1:1 M:L stoichiometry. These findings align with the theoretical calculations. Additionally, the conductivity measurements revealed that all the complexes are non-electrolytic[11],as shown in Table 1.

Nuclear Magnetic Resonance of the ligand (H_2L)

They characterized using ^{1}H NMR and ^{13}C NMR spectroscopy andthen identified by proton and carbon nuclear magnetic resonance spectroscopy: the ^{1}H-NMR and ^{13}C-NMR spectra of the new azo dye are shown in Figure 1, showing the chemical shifts of these spectra; ^{1}H nuclear magnetic resonance 2.42-2.46-2.51 ppm(DMSO-d_6)3.34 ppm(DHO)7.51-7.93 ppm(2CH,m,2H)8.81-8.83-8.85 ppm(3CH(beside azo group),m,3H)10.25 ppm(OH-Phenol,s,H)10.48 ppm(OH-quinolin,s,H)d respectively[12];^{13}C-NMR: 173.22 ppm(C1)170.14 ppm(C5)163.38 ppm(C10)158.26 ppm(C8)154.97 ppm(C9)149.11 ppm(C7)146.04 ppm(C13)137.64 ppm(C12)132.64 ppm(C3)127.44 ppm(C11)118.21 ppm(C15)112.97 ppm(C14)106.90 ppm(C2)103.42 ppm(C4)101.32 ppm(C6)76.97 ppm(Chloroform) respectively[9].

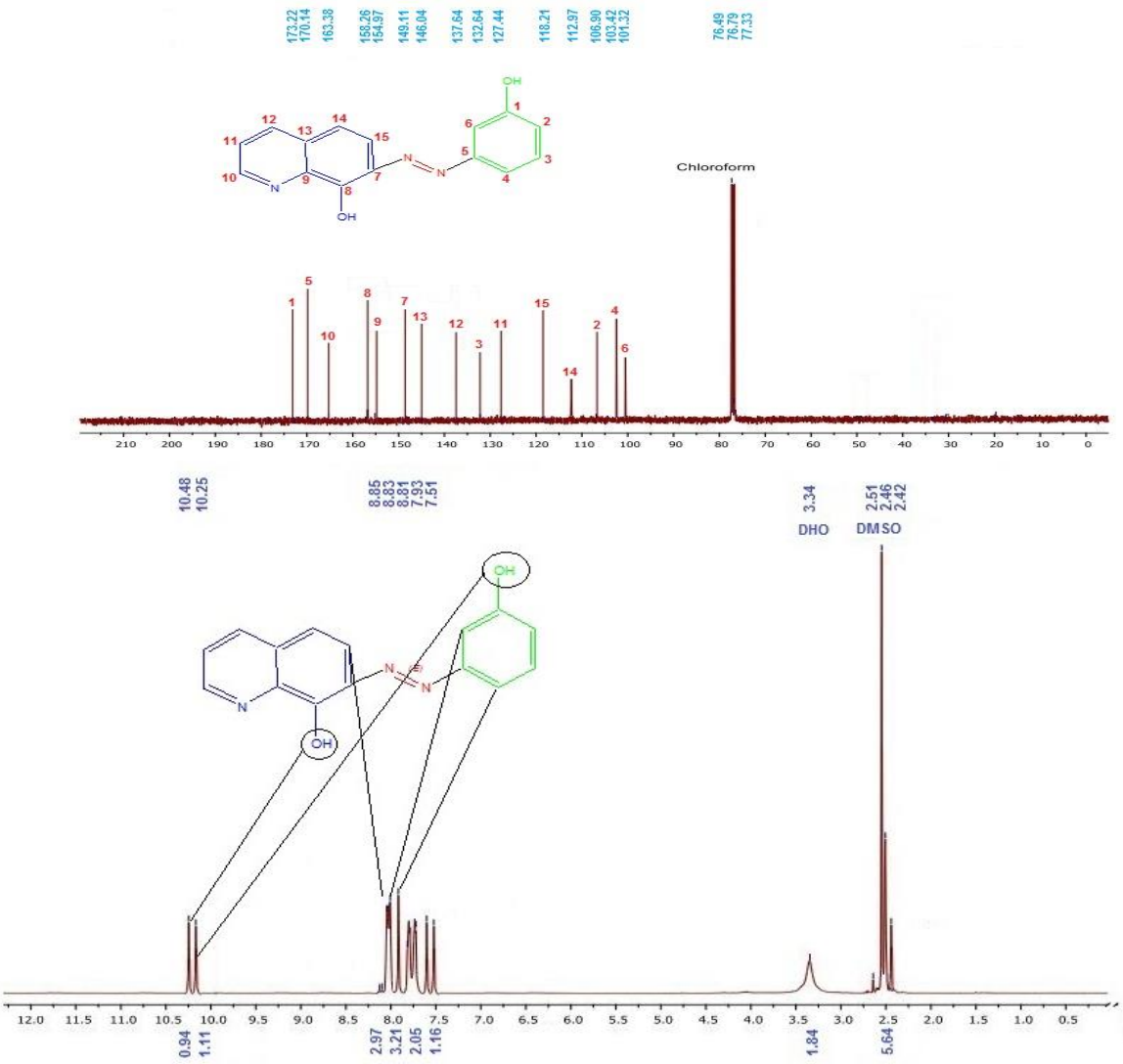

Figure: ^{13}C and ^{1}H-NMR spectra of ligand (H_2L)

Table1: Some elemental physical characteristics investigations of ligand and complexes.

Formula Molecular weight	mp°C	Color		C %	H%	N%	M%	Cl%	Conductivity in DMSOcm^2 $\Omega^{-1}mol^{-1}$
$C_{15}H_{11}N_3O_2$ 265.27	165-167	Reddish brown	Calculated	66.99	3.68	16.97	-	-	
			found	67.09	4.18	15.84	-	-	
$C_{15}H_{11}N_3O_4V$ 348.21	267-269	Blue-green	found	50.97	4.01	13.04	13.60	-	12
			Calculated	51.74	3.18	12.07	14.63	-	
$C_{15}H_{11}N_3O_3Mn$ 372.23	282-284	Brown	found	47.97	4.24	12.20	13.81	-	16
			Calculated	48.40	4.06	11.29	14.76	-	
$C_{15}H_{13}N_3O_4ClCr$ 386.73	>300	Greenish brown	found	45.69	4.12	11.76	13.12	10.02	19
			Calculated	46.59	3.39	10.87	13.45	9.17	
$C_{15}H_{11}N_3O_5Mo$ 409.23	242-244	Reddish brown	found	44.67	2.85	11.31	23.94	-	11
			Calculated	44.03	2.71	10.27	23.45	-	

Mass spectrometry of H_2L and its complexes:

One of the main methods used to characterize ligand (H_2L) and some products is LC mass spectrometry. This method complements other methods that use (m/z) relationships to estimate the molecular weight of chemicals [6]. Scheme 2 shows the mass information of the ligand and its complex, showing the fragmentation pattern and extracted mass for each mode. The molecular ion peak of the $[M]^+$ fragment is visible.$C_{15}H_{10}N_3O^+$Its relative abundance is about 58% in Figure 2, in addition to the remaining peaks including other abundances of $C_6H_4^{+\bullet}$, $C_3H_2N_2O^{2+}$ and $C_6H_5N_1^{\bullet+}$, corresponding to the abundances of 79%, 68%, 37% of Ligand, as shown in Figure 3, illustrates the following fragments: (M^+) has a relative abundance of 17% at 348.68 m/z, and the next pattern is: $C_{15}H_9N_3O_3V^+$, $C_9H_8N_3O_2V^+$, $C_9H_4N_3OV^+$ and $C_6H_3O_2^+$, corresponding to 329.29 m/z, 313.01 m/z, 221.35 m/z and 91.49 m/z, respectively. The $[Mo(L)H_2O]$ complex shown in Scheme 2 and Figure 4 illustrates the followingmass spectralfragments: (M^+) has a relative abundance of 17% at 348.68 m/z, and the next pattern is: $C_{15}H_9N_3O_3V^+$, $C_9H_8N_3O_2V^+$, $C_9H_4N_3OV$+ and $C_6H_3O_2^{\bullet+}$, corresponding to 329.29 m/z, 313.01 m/z, 221.35 m/z and 91.49 m/z, respectively. 9%and next pattern,$C_{15}H_8N_3MoO_4^+$,$C_{15}H_8MoN_3O_2^+$and $C_3H_2MoN_2O^{+\cdot}$and$C_6H_4N^+$., whichcorresponded to 390.69m/z,358.47m/z ,180.15m/z, and 90.67m/z [10,12].

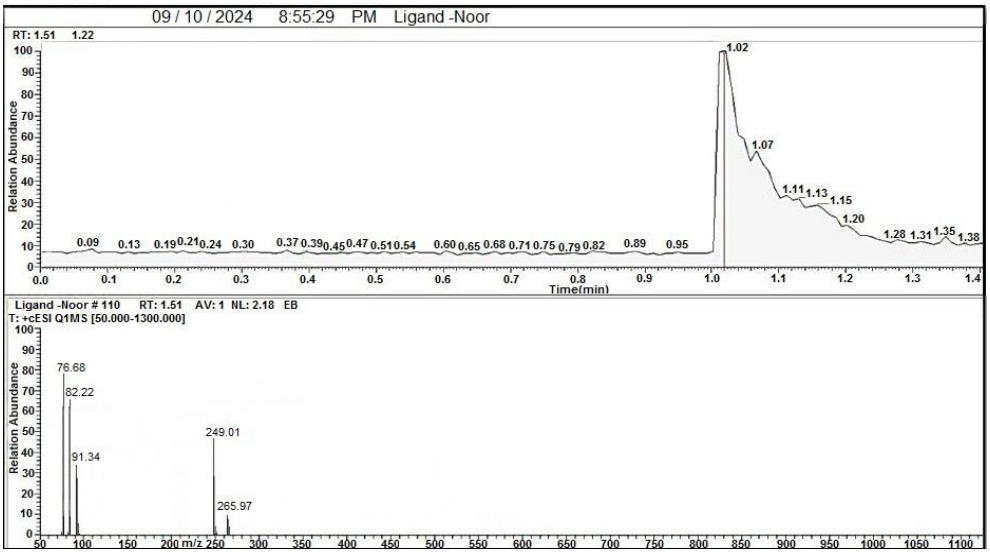

Figure2: Mass spectrum of ligand H_2L

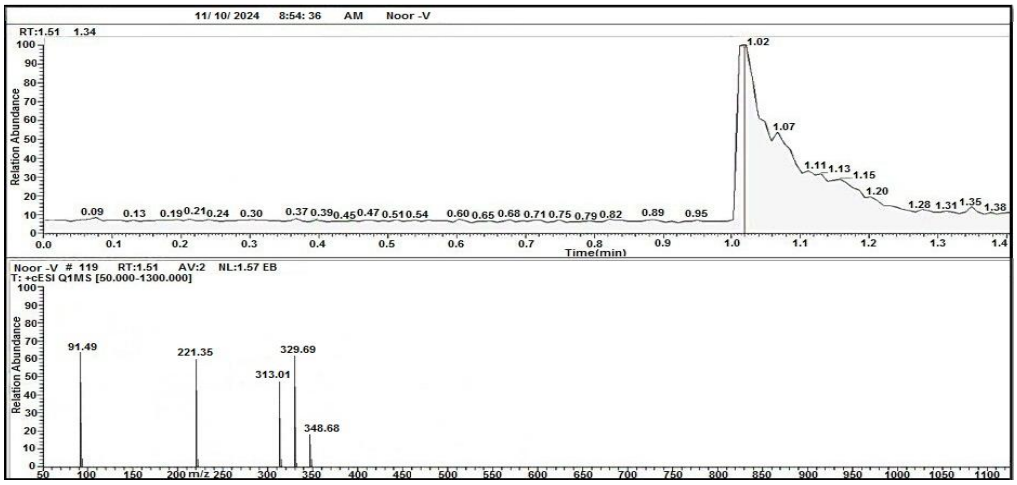

Figure3: Mass spectrum of V-complex

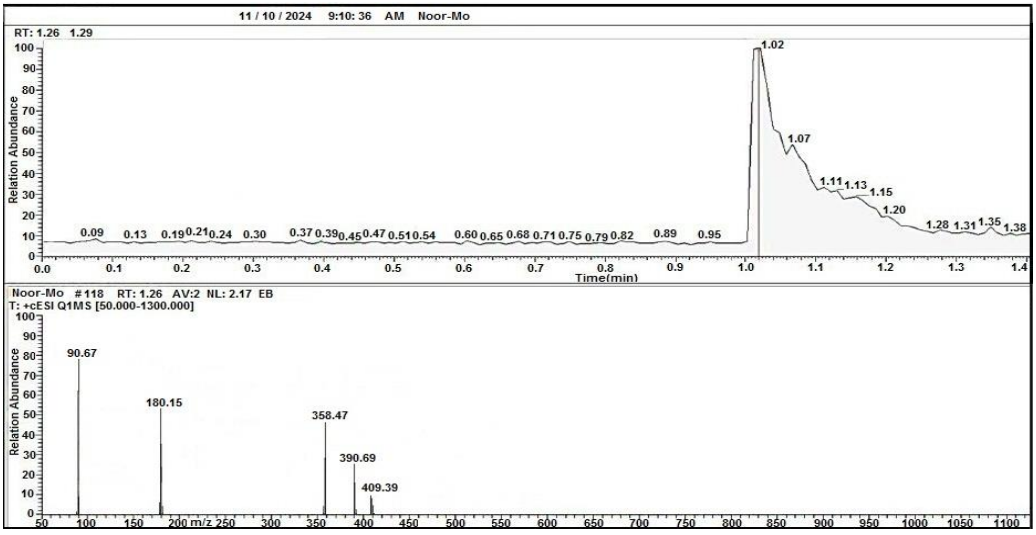

Figure4: Mass spectrum of Mo-complex

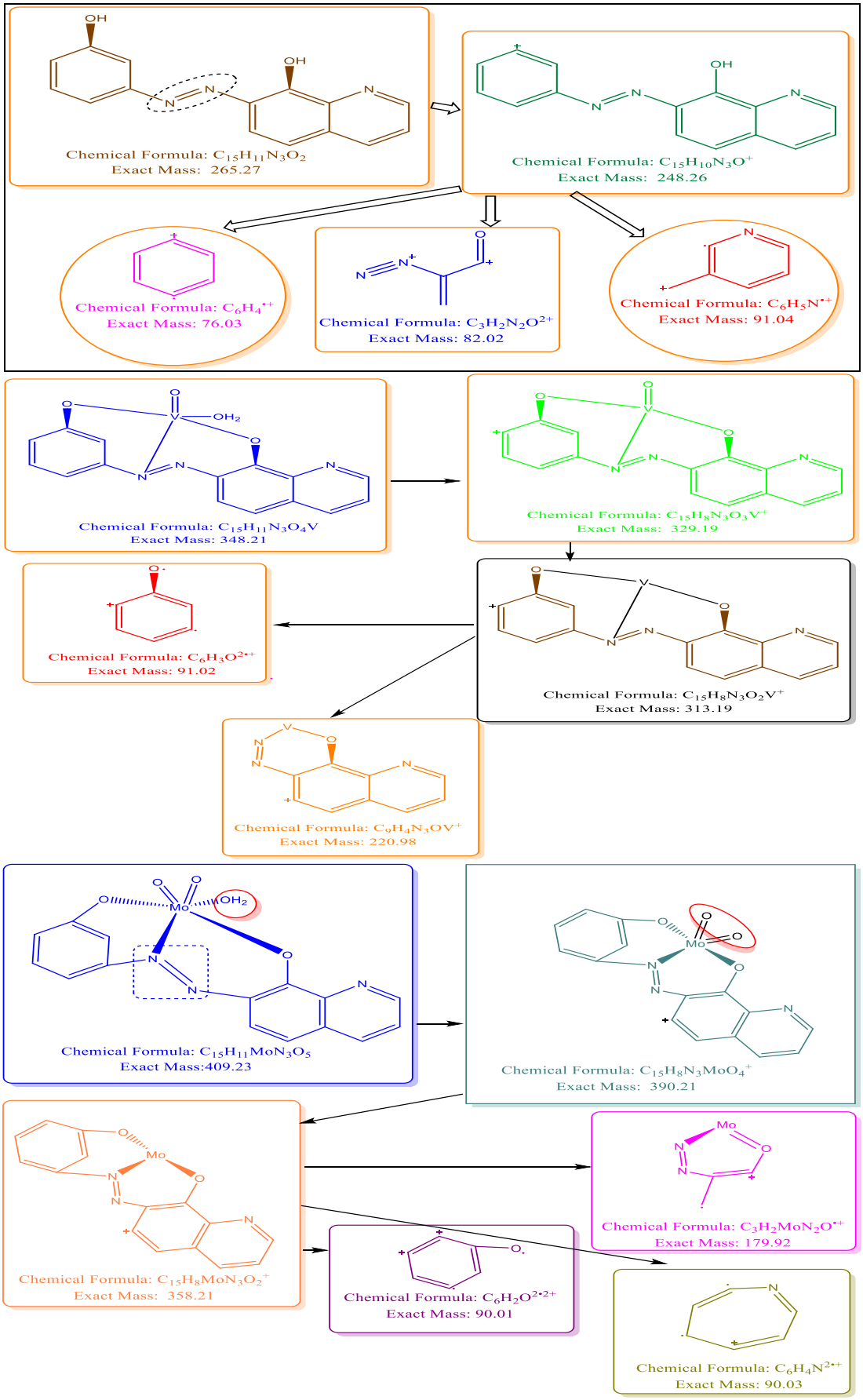

Scheme 2: Pattern of Fragmentation of Ligand,V-complex and Mo-complex.

Ultraviolet-visible spectroscopy (UV-Vis) the ligand (H_2L) and its complex

The electronic spectrum of the ligand (H_2L) in Figure 5 and Table 2 shows a strong absorption at (268 nm, 37313.43 cm^{-1}) due to the $\pi \longrightarrow \pi^*$ transition and a peak at (378 nm, 26455.02 cm^{-1}) attributed to the $n \longrightarrow \pi^*$ transition, and a peak at (424 nm, 23584.91 cm^{-1}) attributed to the C.TLL transition, where a high-intensity band is formed with an absorption maximum [13]. The electronic transitions of the V(IV) complex shown in Figure 6 and Table 2 show that the peaks at (205, 273, 320, 540 and 632) nm corresponding to $\pi \rightarrow \pi^*$, $n \rightarrow \pi^*$, C.TLM $^2B_2g \rightarrow {}^2B_1g$ are assigned to $^2B_2g \rightarrow {}^2Eg$, indicating a square pyramid geometry representation[14]**.**The electronic spectrum of the Cr (III) complexis shown in Figure 7andTable 2, the compound was studied, and itshowedfour peaks, each belonging to the ligand spectrum, a peak in (295,484,581 and 661)nm assigned to $\pi \rightarrow \pi^*$,$n \rightarrow \pi^*$+C.TML,$^4A_2g \rightarrow {}^4T_1g_{(F)}and^4A_2g \rightarrow {}^4T_2g_{(F)}$, this indicates an octahedron [15]. The electronic absorption peaks of the Mn(II) complex in Figure 8 are 260nm , 378 nm, (510, 538)nm and(612, 642 and 676) nm, corresponding to $\pi \rightarrow \pi^*$, $n \rightarrow \pi^*$+ C.TML, $^6A_1g \rightarrow {}^4T_2g(G)$ and$^6A_1g \rightarrow {}^4T_1g$, respectively, indicating anoctahedral[16]. The electronic transitions of the Mo(VI) complex show peaks at (264, 337 and 525) nm, assigned to $\pi \rightarrow \pi^*$, $n \rightarrow \pi^*$ and C.TLM, respectively, indicating an octahedral geometry.Table 2 presents the electronic configurations and corresponding metal complexes[17].

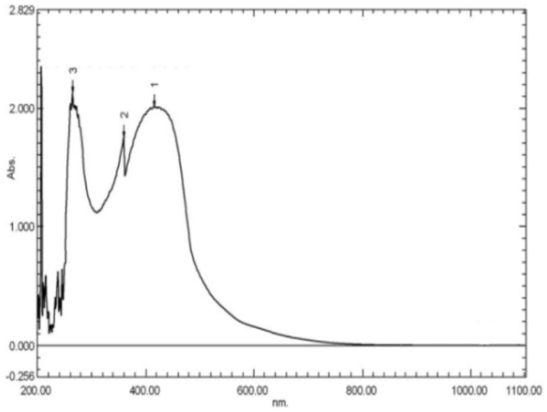

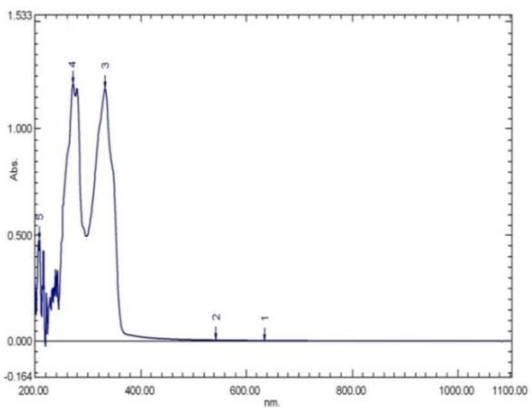

Figure5: UV-Vis spectrum of ligand (H_2L) **Figure6**: UV-Vis spectrum of V-complex

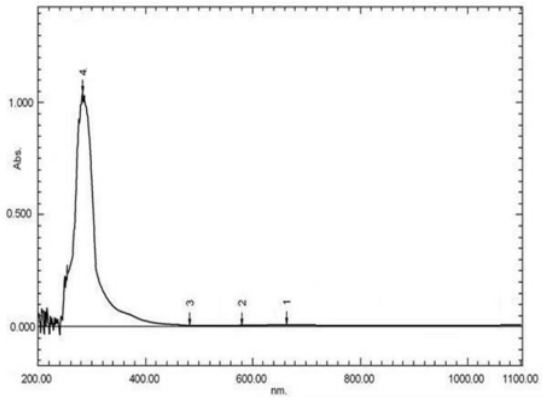

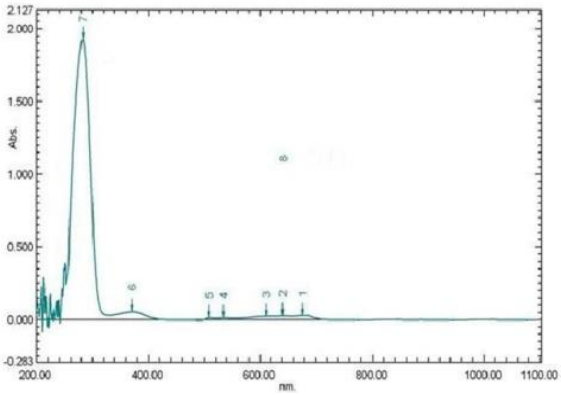

Figure 7: UV-Vis spectrum of Cr-complex **Figure8:** UV-Vis spectrum of Mn-complex

Table 2: The ligand (H_2L) and its complexes are studied by UV-Vis (in $1x10^{-3}$M DMSO)**.**

Compound geometric shape	λ nm	ύcm^{-1}	Abs	ε_{max}Lmol^{-1} cm^{-1}	Assignment	μ_{eff} (B. M)	Hybridization	distribution
Ligand H_2L	268 378 424	37313.43 26455.02 23584.91	2.03 1.72 1.98	2030 1720 1980	π →π* n→ π* C.TLL			
[VO(L)H_2O] Square pyramidal	205 273 320 540 632	48780.48 36630.03 31250 18518.51 15822.78	1.452 1.219 1.183 0.030 0.019	1452 1219 1183 30 19	π→π* π →π* C.TLM $^2B_2g\rightarrow{}^2B_1g$ $^2B_2g \rightarrow {}^2Eg$	1.81	dsp^3	$T_2g^1eg^0$
[Mn(L)(H_2O)$_3$] Octahedral	260 378 510 538 612 642 676	38461.53 26455.02 (19607.84+18587.36) =19097 (16339.86+15576.32+14792.89)= 15569	1.919 0.054 0.012 0.009 0.020 0.022 0.025	1919 54 12 9 20 22 25	π →π* n→ π*+C.TML $^6A_1g\rightarrow{}^4T_2g$ $^6A_1g\rightarrow{}^4T_2g$	5.44	sp^3d^2	$T_2g^3eg^2$
[Cr(L)(H_2O)$_2$Cl] Octahedral	295 484 581 661	33898.30 20661.15 19607.84 15128.59	1.26 0.015 0.018 0.021	1260 15 18 21	π →π* n→π*+C.TLM $^4A_2g\rightarrow{}^4T_1g(F)$ $^4A_2g\rightarrow{}^4T_2g(F)$	3.87	d^2sp^3	$T_2g^3eg^0$
[Mo(L)O_2(H_2O)] Octahedral	264 337 525	37878.78 29673.59 19047.61	2.799 2.111 0.133	2799 2111 133	π →π* n→ π* C.TLM	diamagnetic	sp^3d^2	$T_2g^0eg^0$

Thermalanalysis

Thermal analysis data for the ligand (H_2L) and its synthesized complexes are detailed in Tables 3 and 4, alongside corresponding results illustrated in Figures 9 and 10[9,18]. Schemes 3 outlines the potential breakdown response of metal complexes. Based on the thermograms, computations of the decomposition phases, The thermal range, decomposition products, and weight loss percentage of the compounds showed good agreement between the theoretical and practical calculations, as shown in Table 4. This confirms the proposed formulas for the compounds and the thermal decomposition equation is shown in Scheme 3. It was found that in the ligand the remaining compound is carbon and metal complexes V(IV), Mn(II) and the remaining metal oxide[19,26]. Thermogravimetric experiments showed that the complex and ligand separated into (one to three phases). Using the DCS curve, the thermodynamic parameters enthalpy ΔH, entropy ΔS and Gibbs free energy (ΔG) were calculated, the Mn-complex ΔH= 1.56 J/g exothermic and-0.79,-3.78 J/g endothermic, ΔS= 0.117,-0.250,-0.363 J, and ΔG= 14.713,-39.192,-112.22 J,asshown in (Figure 10)Table3DSCandTGA for Mn complex, and V- complex ΔH= -39.49,-17.48,-2.19J/g endothermic and 236.48J/g exothermic, ΔS= -0.585,-0.383,-0.125,2.521 J, and ΔG= 0.372,40.272,21.241,412.601 J show in Table3 [9,29]**.**

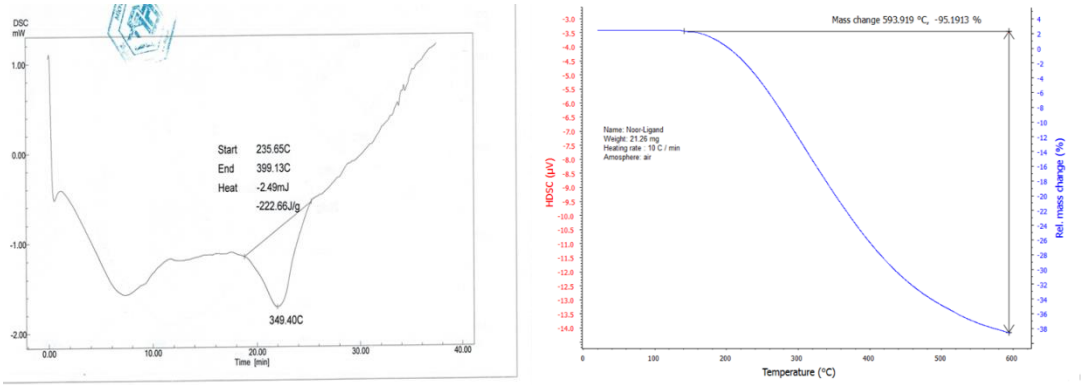

Figure 9: DSC &TGA curve of Ligand (H_2L)

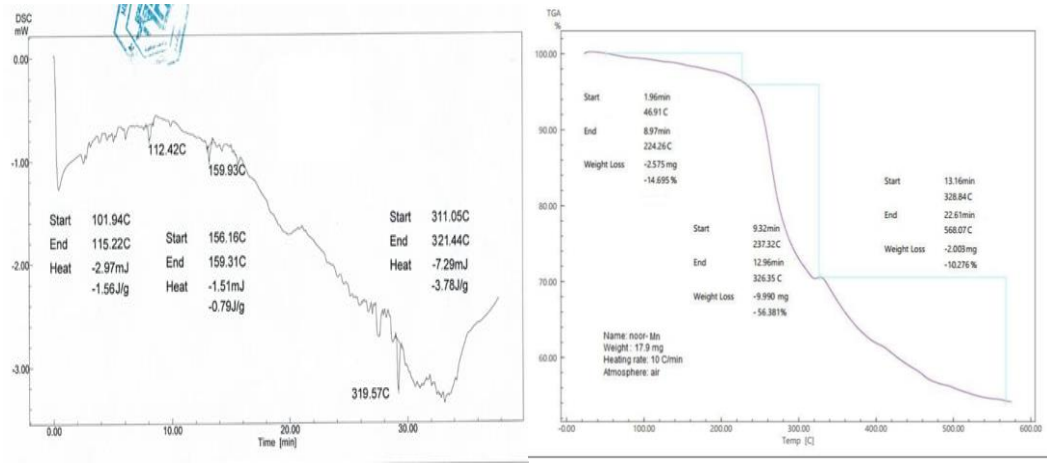

Figure 10: DSC &TGA- curve of Mn-Complex

Table 3:DSC analysis of thermal decomposition of the ligand and its complexes.

compound	T_{i} /°C	T_{f}/°C	Maximum temperature point°C	ΔH J/g	ΔS J	ΔG J	Type
H_2L	235.65	399.13	349.40	-222.66	-1.362	153.22	endothermic
$[Mn(L)(H_2O)_3]$	101.94 156.16 311.05	115.22 159.31 321.44	112.42 159.93 319.57	1.56 -0.79 -3.78	0.117 -0.250 -0.363	14.713 -39.192 -112.22	exothermic endothermic endothermic
$[VO(L)H_2O]$	40.52 128.85 181.36 214.64	108.02 174.48 198.87 308.41	66.87 150.79 187.45 257.47	-39.49 -17.48 -2.19 236.48	-0.585 -0.383 -0.125 2.521	0.372 40.272 21.241 412.601	endothermic endothermic endothermic exothermic

Table 4: TGA data of the ligand H_2Landsome complexes

Compound	**Step**	**T_i/°C**	**T_f/°C**	**Weight mass loss%**		**Reaction**
				Calc	Found	
Ligand	1	157.26°C	593.919°C	95.4763%	95.1913%	$C_{14}H_{11}N_3O_2$
						C
Calculated: 95.48% , Final=4.524%, Estimated=95.1913%, Final=4.808%						
$[Mn(L)(H_2O)_3]$	1	46.91°C	224.26°C	14.501%	14.695%	$-3H_2O$
	2	237.32°C	328.84°C	56.381%	56.381%	$-C_{12}H_7N_3O$
	3	328.84°C	568.07°C	10.208%	10.276%	$-C_3H_4N_2$
	4	440.948°C	545.451°C	14.07035%	13.41831%	$-C_5H_2$
						-MnO
Calculated: 95.1603%, Final=4.839%, Estimated:94.7703%, Final=5.229%						
$[VO(L)H_2O]$	1	97.80°C	395.60°C	53.703%	53.260%	$-H_2O$,- $C_{11}H_9N_2$
	2	242.54°C	571.12°C	26.995%	25.942%	$-C_4NO_2$
						VO^{+2}
Calculated: 80.70%, Final=19.30%, Estimated79.20%, Final=20.80%						

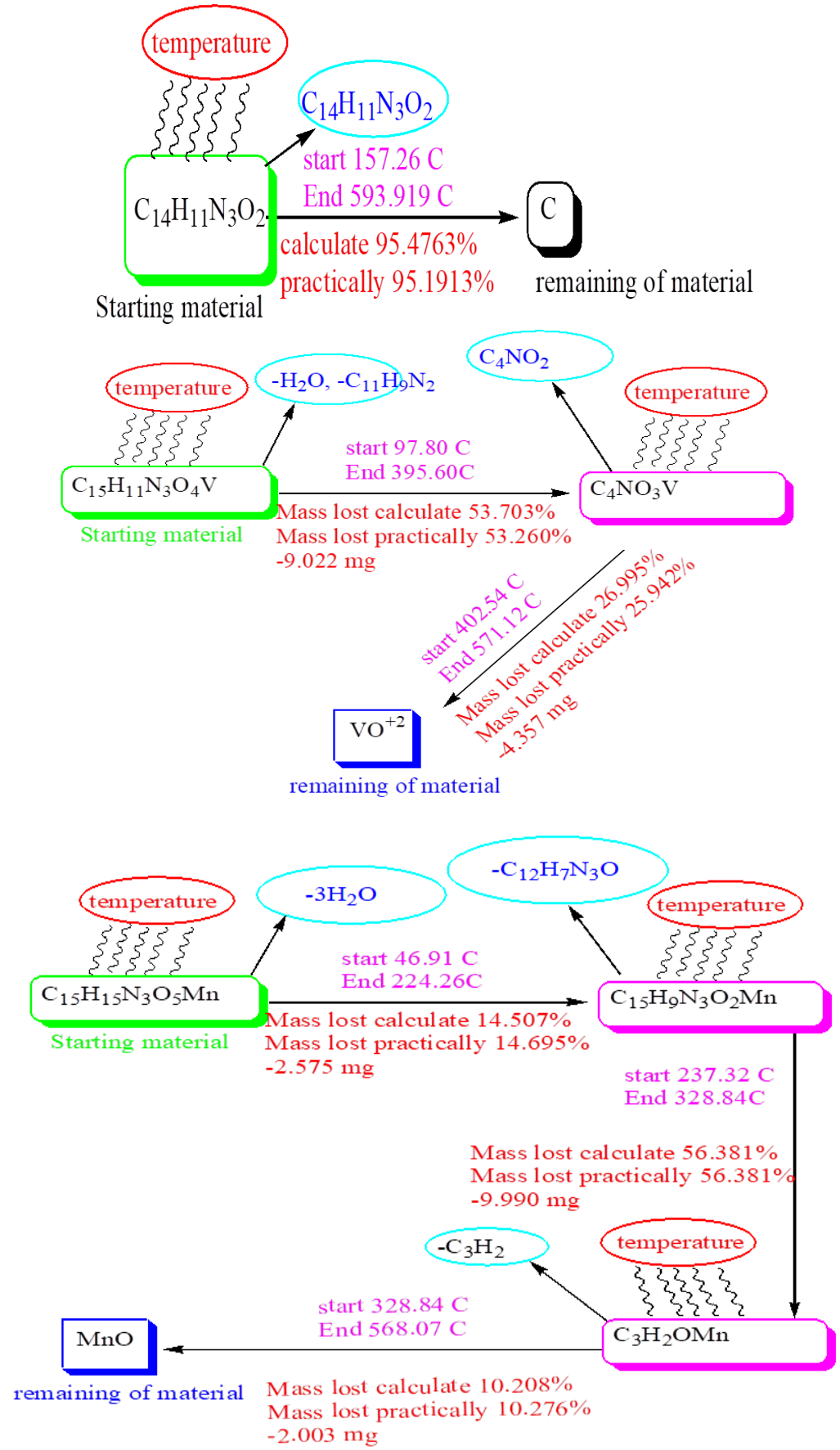

Scheme 3: Preliminary breakdown reactions of metal complexes and their ligand.

Fourier-transform infrared spectroscopy (FTIR):

The infrared spectra of ligand H_2L and its metal complexes were recorded withCr(III), V(IV), Mn(II) and Mo(VI). The data of the ligand are collated in Table 5 and Figure 11, and the data of the complexesCr(III), V(IV) and Mo(VI)are collated in Figures 12 and 13. The ligandshows bands at 3051, 1139, and 1381 cm^{-1}, which are assigned to ν (C-H) aromatic, ν (C-O), and ν (N=N) [20]. Subsequently, the infrared spectra of all the created compounds showed that the azo dye ligandis coupled to the metal ions through two sites: the deprotonated oxygen site of the phenol group and the nitrogen site of the azo group [18]. New bands belonging to (M-N) appearedat (528, 580 and,452, 517and 580) cm^{-1} for the Cr(III), V(IV), Mn(II) and Mo(VI) complexes, respectively, (M-O) at (451, 432, 462 and 478) cm^{-1} for the complexes ofCr(III), V(IV), Mn(II) and Mo(VI) respectively, (V=O) at (968) cm^{-1} for the complex of V(IV) and (Mo=O) at (1155) $cm^{-1}$for the Mo(VI) complex[21,27,28].

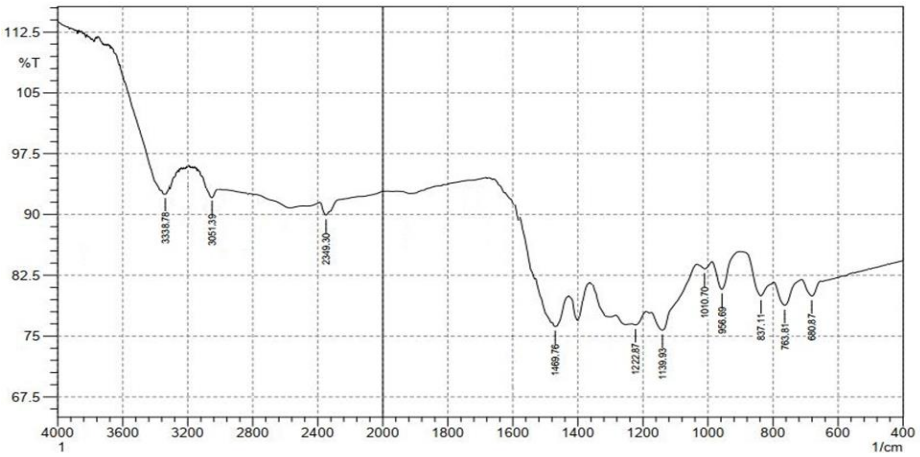

Figure 11: FT-IR Spectrum of Ligand (H_2L)

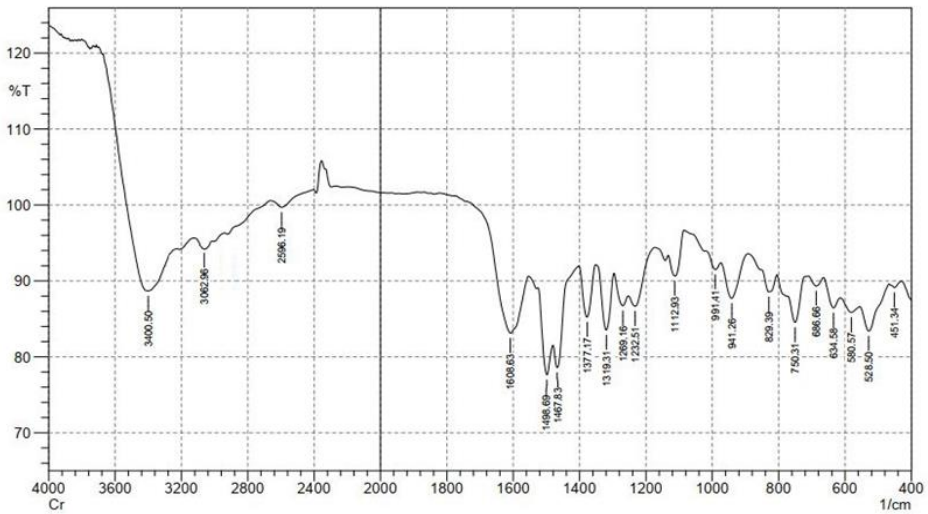

Figure12: FT-IR Spectrum of Cr complex

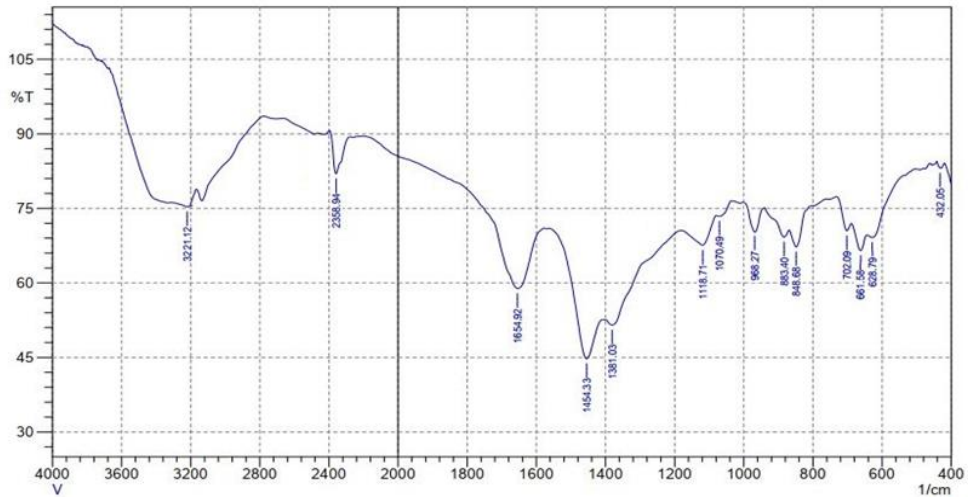

Figure 13: FT-IR spectra of V complex

Table 5: Infrared spectral bands of ligand and their complexes (cm^{-1})

Compound	ν (H_2O) aqua	ν(C-H) aromatic	ν (C-O)	ν (N=N)	Other bands
H_2L	-	3051	1139	1381	
$[Mn(L)(H_2O)_3]$	3383,1641 837	3015	1217	1409	517(Mn-N) 462(Mn-O)
$[VO(L)H_2O]$	3221, 1654 848	3120	1118	1454	432(V-N) 452(V-O), 968 (V=O)
$[Cr(L)(H_2O)_2Cl]$	3400, 1608 829	3062	1269	1467	451(Cr-N) 528, 580(Cr-O)
$[Mo(L)O_2(H_2O)]$	3334, 1624 831	3147	1234	1408	580(Mo-N), 478(Mo-O) 1155(Mo=O)

Evaluation of Antioxidant Activity

The antioxidant activity of H_2L and its mineral complexes was measured by Gallicacid and the DPPH assay was used to scavenge free radicals.Each sample was initially diluted with an equal volume of methyl alcohol, then mixed with an identical volume of concentrated 0.135 mMDPPH solution. Following the addition of the DPPH solution, the mixtures were kept at room temperature in the dark for 30 min. The absorbance of each sample was then measured at 517 nm. The lower the IC_{50} value of the complex, the stronger its ability to inhibit free radicals compared to gallic acid, because the ligand is the strongest free radical inhibitor, followed by gallic acid, followed by molybdenum complexes, vanadium complexes, and manganese [8,9,13,20]. The IC_{50} values were lower and the results were as follows (H_2L> Gallic acid>Mo-complex> V-complex and Mn-complex),as shown in Figure 14and Table 6.

Table6: The antioxidant results (P1%, RSA% and IC_{50}) of H_2L and its complexes.

compound	Concentration µ/mL	PI%	RSA%	IC_{50}µ/mL
Ligand	0.080	22.06	77.94	0.020
	0.040	47.99	52.01	
	0.020	56.16	43.84	
	0.010	64.95	35.05	
	0.005	70.71	29.29	
Gallic acid	0.080	18.73	81.27	0.021
	0.040	45.69	54.31	
	0.020	60.35	39.65	
	0.010	68.16	31.84	
	0.005	72.36	27.64	
$[Mo(L)O_2(H_2O)]$	0.080	11.36	88.64	0.029
	0.040	20.33	79.67	
	0.020	27.06	72.94	
	0.010	29.95	70.05	
	0.005	32.05	67.95	
$[VO(L)H_2O]$	0.080	24.09	75.91	0.031
	0.040	35.75	64.25	
	0.020	44.16	55.84	
	0.010	47.62	52.38	
	0.005	49.68	50.32	
$[Mn(L)(H_2O)_3]$	0.080	14.61	85.39	0.031
	0.040	19.64	80.36	
	0.020	23.09	76.91	
	0.010	25.64	74.36	
	0.005	26.12	73.88	

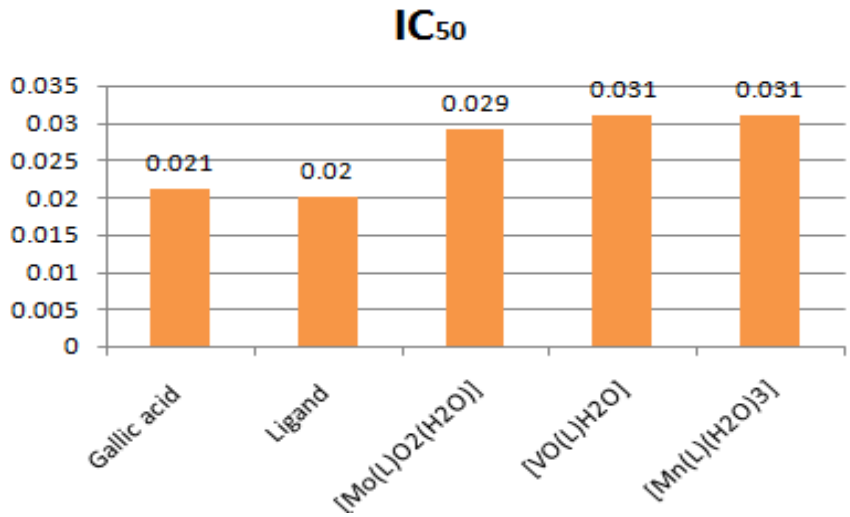

Figure 14: The differences in IC_{50} values observed for Gallic acid and its metal complexes

Evaluation of Anticancer Activity

Cancer cell growth was determined using MTT, and MCF-7 cells were digested with trypsin. The cells were treated with five concentrations 7.4-600 µg/ml with complexes for 24 hours at 37 °C in 5 % CO_2, and the MTT solution was added in phosphate-buffered saline for an additional four hours, and the absorbance was determined as 570nm. Using an ELISA reader, and the concentration of complexes V-Complex in Table 7, Figure15 and Mo-Complex Table-8, Figure 16 that led to 50% of cell death was determined [10,22,24,25,30], The inhibitory capacity of the complexes was determined after comparing them with the cis-platin complex Figure 17 Table 9, which was studied in the same way and under the

conditions of the complexes. The results of the two complexes gave positive results. The reason can be attributed to the fact that the quaternary vanadium and hexagonal molybdenum can oxidize and reduce and possess the oxo group.

Table 7: Cellular toxicity of vanadium complex towards MCF-7

Control (untreated sample) average absorption at 570 nm							
Sample ID	Concentration (µg/mL)	Absorption at 570 nm		Viability (%)		Average Viability (%)	Standard Deviation (±)
NAT-5 MCF-7 24 h	7.4	0.254	0.294	86.44	81.80	84.12	0.68
	22.22	0.244	0.212	79.64	84.00	81.82	0.64
	66.66	0.168	0.159	61.82	65.24	63.53	1.60
	200	0.121	0.128	31.02	28.34	29.68	0.38
	600	0.054	0.061	12.64	15.60	14.12	2.17
IC_{50} = 97.62 µg/mL , a= -0.108x , b = 71.32, R^2= 0.689							

Table 8: Cellular toxicity ofmolybdenum complex towards MCF-7

Control (untreated sample) average absorption at 570 nm							
Sample ID	Concentration (µg/mL)	Absorption at 570 nm		Viability (%)		Average Viability (%)	Standard Deviation (±)
NAT-7 MCF-7 24h	7.4	0.338	0.333	99.41	97.94	98.68	1.04
	22.22	0.327	0.323	96.18	95.00	95.59	0.83
	66.66	0.297	0.307	87.35	90.29	88.82	2.08
	200	0.273	0.256	80.29	75.29	77.79	3.54
	600	0.100	0.107	29.41	31.47	30.44	1.46
IC_{50} = 40.08 µg/mL, a=-0.112x, b= 98.47 , R^2= 0.997							

Table 9: Cellular toxicity of Cis-platin complex towards MCF-7

Sample ID	Concentration (µg/mL)	Absorption at 570 nm		Viability (%)		Average Viability (%)	Standard Deviation (±)
Cis-Platin MCF 7 24 h	7.4	0.338	0.326	91.29	94.05	92.67	0.82
	22.22	0.325	0.317	88.61	87.35	87.98	0.63
	66.66	0.307	0.305	82.67	86.61	84.64	0.39
	200	0.288	0.292	78.94	76.40	77.67	2.31
	600	0.257	0.226	66.23	63.11	64.67	9.84
IC_{50} = 34.08 µg/mL, a=-0.042x, b= 89.19 , R^2= 0.942							

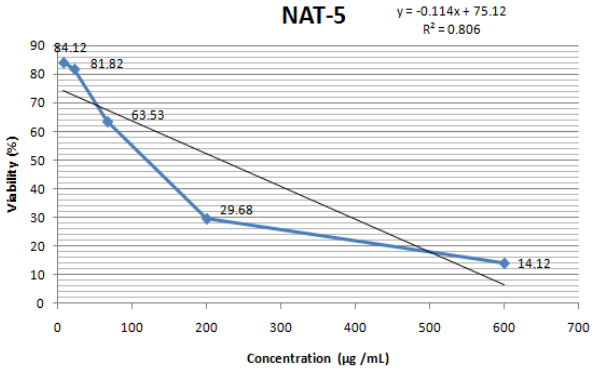

Figure15: Cytotoxicity of V complex vs. MCF-7

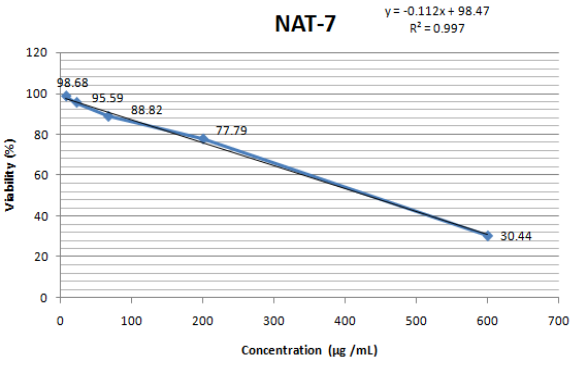

Figure16: Cytotoxicity of Mo complex

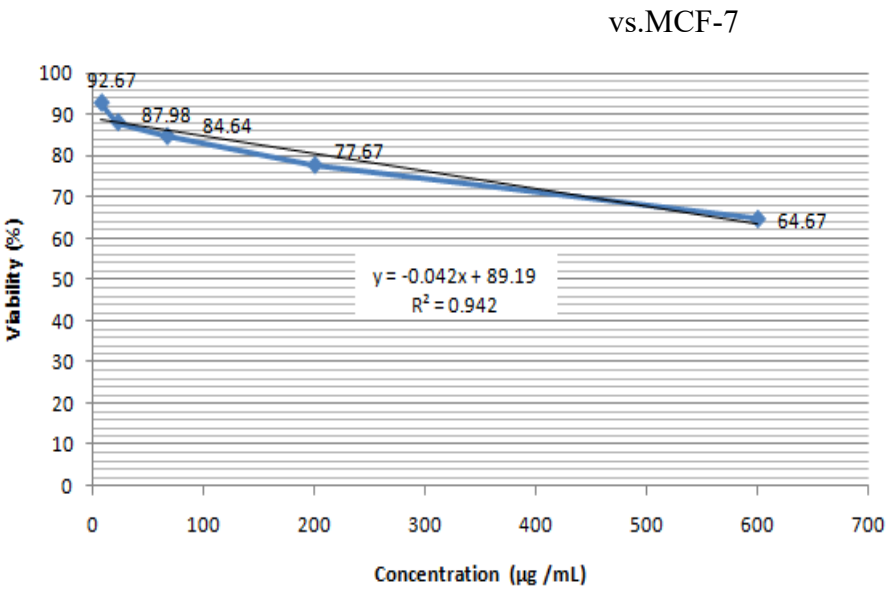

Figure17: Cytotoxicity of cis-platin complex vs.MCF-7

Conclusion

Through diazotization of 3-aminophenol followed by coupling with 8-hydroxyquinoline, a novel azo derivative was synthesized and subsequently used to prepare metal complexes with vanadium, chromium, manganese, and molybdenum. The compounds were identified using various analytical and diagnostic methods, careful analysis of elements, and elemental analysis, metal chlorides, conductivity measurements, magnetic susceptibility, ^{1}H and $^{13}CNMR$, FT-IR and UV-Vis spectroscopy including thermal analysis curves (TGA and DSC), the thermodynamic parameters ΔH, ΔS and ΔG were calculated using DCS curves. The triple coordination sites of the N , O, and O atoms in the ligand were determined by comparing the IR spectra with those of the metal complexes.The M:L ratio for each complex was [1:1]. It usedligands and complexes to determine their ability to inhibit free radicals using its antioxidant ability was determined using DPPH as a free radical and gallic acid as a standard substance. The IC_{50} value was determined and it was found that the ligand had a high free radical inhibition ability. The free radical inhibition ability and complex inhibition ability varied according to the IC_{50} value, and the results were as follows ((H_2L>gallic acid > Mo complex > V complex and Mn complex), The effectiveness of vanadium and molybdenum complexes as anti-cancer agents against breast cancer was evaluated MCF-7, and the results were compared with the cis-platin complex. The effectiveness results showed the highest effectiveness of the molybdenum complex after thecis-platin complex and then the vanadium complex.

References

[1] I. H. Ibraheem, N. S. Mubder, M. M. Abdullah, and H. Al-Neshmi, "Synthesis, characterization and bioactivity study from azo-ligand derived from methyl-2-amino benzoate with some metal ions," *Baghdad Science Journal*, vol. 20, no. 1, pp. 0114–0114, 2023.

[2] N. Nagasundaram, C. Govindhan, S. Sumitha, N. Sedhu, K. Raguvaran, S. Santhosh, and A. Lalitha, "Synthesis, characterization and biological evaluation of novel azo fused 2,3-dihydro-1H-perimidine derivatives: In vitro antibacterial, antibiofilm, anti-quorum sensing, DFT, in silico ADME and molecular docking studies," *Journal of Molecular Structure*, vol. 1248, art. no. 131437, 2022.

[3] S. D. Al-Qahtani, R. B. Alnoman, N. M. Alatawi, K. M. Alkhamis, A. Bayazeed, A. Alsoliemy, and N. M. El-Metwaly, "Improvement of dye-sensitized solar cells' performance via co-

sensitization of new azo thiazole organic dyes with ruthenium (II) based N-719 dye," *Journal of Saudi Chemical Society*, vol. 27, no. 3, pp. 101643, 2023.

[4] M. H. Alhalafi, "Novel azo-dye quinazolinones as colorimetric chemosensors for detection of cobalt and ferrous ions in aqueous medium," *Journal of Saudi Chemical Society*, vol. 27, no. 4, pp. 101685, 2023.

[5] M. Lashanizadegan, H. A. Ashari, M. Sarkheil, M. Anafcheh, and S. Jahangiry, "New Cu(II), Co(II) and Ni(II) azo-Schiff base complexes: Synthesis, characterization, catalytic oxidation of alkenes and DFT study," *Polyhedron*, vol. 200, art. no. 115148, 2021.

[6] J. Keshavayya, I. Pushpavathi, C. T. Keerthikumar, M. R. Maliyappa, and B. N. Ravi, "Synthesis, characterization, computational and biological studies of nitrothiazole incorporated heterocyclic azo dyes," *Structural Chemistry*, vol. 31, no. 4, pp. 1317–1329, 2020.

[7] C. Keshava et al., "Application of systematic evidence mapping to identify available data on the potential human health hazards of selected market-relevant azo dyes," *Environment International*, vol. 176, art. no. 107952, pp. 1–12, 2023.

[8] H. S. Mohammed, H. A. Al-Hasan, Z. Chaieb, Z. Zizi, and H. N. Abed, "Synthesis, characterization, DFT calculations and biological evaluation of azo dye ligand containing 1,3-dimethylxanthine and its Co(II), Cu(II) and Zn(II) complexes," *Bulletin of the Chemical Society of Ethiopia*, vol. 37, no. 2, pp. 347–356, 2023.

[9] K. A. Hussein, S. Mahdi, and N. Shaalan, "Synthesis, spectroscopy of new lanthanide complexes with Schiff base derived from (4-antipyrinecarboxaldehyde with ethylene di-amine) and study the bioactivity," *Baghdad Science Journal*, vol. 20, no. 2, pp. 469–482, 2023.

[10] B. N. Ravi, J. Keshavayya, V. Kumar, and S. Kandgal, "Synthesis, characterization and pharmacological evaluation of 2-aminothiazole incorporated azo dyes," *Journal of Molecular Structure*, vol. 1204, art. no. 127493, 2020.

[11] W. J. Geary, "*The use of conductivity measurements in organic solvents for the characterisation of coordination compounds,*" *Coordination Chemistry Reviews*, vol. 7, pp. 81–122, 1971.

[12] R. M. Silverstein, G. C. Bassler, and T. C. Movril, *Spectroscopic Identification of Organic Compounds, 4th ed., New York: Wiley*, 1981.

[13] M. Hasan, "Synthesis, Identification, and Biological Study for Some Complexes of Azo Dye Having Theophylline", *The Scientific World Journal*, vol. 2021, pp. 1-9, 2021.

[14] F. Sh. H. Al-Zahraa and A. A. S. Al-Hamdani, "Synthesis, characterization, thermal studies, and antioxidant activities of azo dye [2-[(3-hydroxyphenyl)diazinyl]-1,2-benzothiazol-3(2H)-one-1,1-dioxide] and metal ion complexes," *Iraqi Journal of Science*, vol. 65, no. 12, pp. 6842–6861, 2024.

[15] E. S. Mahdi and A. J. Alabdali, "Synthesis, characterization and anti-bacterial activity of mono and binuclear Co(II) and Cr(III) mixed-ligand complexes derived from alpha-amino acid and 1,10-phenanthroline with 1,3-diaminopropan as a spacer," *Journal of Polymer Composites*, vol. 11, Special Issue 2, pp. S107–S117, 2023.

[16] N. Shaalan, W. M. Khalaf, and S. Mahdi, "Preparation and characterization of new tetra-dentate N2O2 Schiff base with some of metal ions complexes," *Indonesian Journal of Chemistry*, vol. 22, no. 1, pp. 62–71, 2022.

[17] A. B. P. Lever, *Inorganic Electronic Spectroscopy, 6th ed., Amsterdam, London: Elsevier Publishing Company*, 1968, p. 121.

[18] N. Asim, MH Amin, MA Alghoul, SN Sulaiman, H Razali, M Akhtaruzzaman, N Amin, K Sopian, "Developing of chemically treated waste biomass adsorbent for dye removal", *Journal Natural Fibers*, vol.8, no. 7, p. 968-977, 2021

[19] R. Kh. H. Al-Daffaay, "Preparation, spectroscopic characterization of transition metal complexes with Schiff base 2-[1-(1H-indol-3-yl)ethylimino)methyl]naphthalene-1-ol," *Baghdad Science Journal*, vol. 20, no. 7, pp. 1036–1044, 2022.

[20] M. M. Reda and L. A. Mohammed, "Preparation, characterization and studied biological effect as antioxidant of azo compound and Schiff base complexes," *Journal of Survey in Fisheries Sciences*, vol. 10, no. 35, pp. 1144–1156, 2023.

[21] A. Unnisa, A. S. Abouzied, A. Baratam, K. C. Lakshmi, T. Hussain, R. D. Kunduru, and K. K. Selvarajan, "Design, synthesis, characterization, computational study and in-vitro antioxidant and

anti-inflammatory activities of few novel 6-aryl substituted pyrimidine azo dyes," *Arabian Journal of Chemistry*, vol. 13, no. 12, pp. 8638–8649, 2020.

[22] S. Benkhaya, S. Mrabet, and A. Elharfi, "Classifications, properties, recent synthesis and applications of azo dyes," *Heliyon*, vol. 6, art. no. e03271, pp. 1–26, 2020.

[23] R. M. Al-Ezzy, A. F. Alshanon, and H. M. Khalaf, "Studying some cytotoxic and cytogenetic potentials of Dandelion methanolic extract on MCF-7 cancer cell line: an in vitro study," *Iraqi Journal of Science*, pp. 1160–1170, 2023.

[24] H. A. El-Ghamry, A. A. Alkurbi, M. A. Alhasani, K. M. Takroni, and A. M. Khedr, "Copper based azo dye catalysts for phenoxazinone synthase mimicking efficiency structure characterization and bioactivity evaluation," *Arabian Journal of Chemistry*, vol. 16, no. 8, p. 104916, 2023.

[25] A. M. Abdullah and A. A. S. Al-Hamdani, "Synthesis, characterization, thermal studies and antioxidant activities of transition metal complexes with azo dye ligand," *Baghdad Science Journal*, vol. 21, pp. 1512–1535, 2024.

[26] M. Abd El-Lateef, M. Khalaf, A. Amer, M. Kandeel, A. Abdelhamid, and A. Abdou, "Synthesis, characterization, antimicrobial, density functional theory, and molecular docking studies of novel Mn(II), Fe(III), and Cr(III) complexes incorporating 4-(2-hydroxyphenylazo)-1-naphthol (Az)," *ACS Omega*, vol. 8, pp. 25877–25891, 2023.

[27] D. Akram, I. A. Elhaty, and S. S. AlNeyadi, "Synthesis and spectroscopic characterization of rhodanine azo dyes as selective chemosensors for detection of iron(III)," *Chemical Data Collections*, vol. 28, p. 100456, 2020.

[28] S. Zafar, D. A. Bukhari, and A. Rehman, "Azo dyes degradation by microorganisms–An efficient and sustainable approach," *Saudi Journal of Biological Sciences*, vol. 29, no. 12, p. 103437, 2022.

[29] W. Al Zoubi, V. Jirjees, V. Suleman, Y. G. Kim, A.A.S. Al-Hamdani and Y. G. Ko, "Synthesis and bioactivity studies of novel Schiff bases and their complexes," *Journal of Physical Organic Chemistry*, vol. 32, p. e4004, 2019.